Trop J Nat Prod Res, February 2025; 9(2): 495 - 503 **ISSN 2616-0684 (Print)**
ISSN 2616-0692 (Electronic)

Tropical Journal of Natural Product Research

Available online at https://www.tjnpr.org

Original Research Article

Cytotoxicity of *Blumea balsamifera* on A549 Lung Cancer Cells: Integrating *in Vitro* Analysis with Computational Study of AKT-1 Inhibition

Friska A Nurlailiyah[1], Dinia R Dwijayanti[1,2,3]*, Feri E Hermanto[4], Masruri Masruri[5], Nashi Widodo[1,2]

[1]*Department of Biology, Faculty of Mathematics and Natural Sciences, Brawijaya University, East Java, Indonesia*
[2]*Research Center of Complementary Medicine and Functional Food, Brawijaya University*
[3]*Dewan Jamu East Java Region, Malang, East Java, Indonesia*
[4]*Division of Computational Biology, Faculty of Animal Sciences, Brawijaya University, East Java, Indonesia*
[5]*Department of Chemistry, Faculty of Mathematics and Natural Sciences, Brawijaya University, East Java, Indonesia*

ARTICLE INFO

Article history:
Received 05 September 2024
Revised 09 October 2024
Accepted 04 January 2025
Published online 01 March 2025

ABSTRACT

Lung cancer is the second leading cause of death worldwide, necessitating the exploration of novel therapeutic agents. This research investigates the potential of *Blumea balsamifera* L. extract (BBE) as an anti-lung cancer agent by examining its cytotoxic effects on A549 lung cancer cells and exploring its bioactive compounds' interactions with key target proteins involved in cancer cell growth. A549 cells were treated with BBE at concentrations of 0, 25, 50, and 100 µg/mL, and cytotoxicity was evaluated using the WST-1 assay. In silico analyses were performed, including data mining, bioactivity prediction, protein target identification, molecular docking, and molecular dynamics simulations. The results demonstrated that BBE exhibited cytotoxic activity against A549 cells, with an IC_{50} value of 124.92 ± 13.24 µg/mL. Computational studies supported these findings, indicating that BBE targets the AKT-1 protein, a critical regulator of cancer cell growth and survival. Among the bioactive compounds identified, rutin, eriodictyol, and ombuin showed the strongest binding affinities and stable interactions with AKT-1, suggesting their potential as anticancer agents. This study provides a comprehensive understanding of the cytotoxic effects of BBE on A549 lung cancer cells, validated through both *in vitro* and *in silico* methodologies, and highlights the potential of BBE as a promising therapeutic candidate for lung cancer treatment.

Keywords: A549, AKT-1, Cytotoxic, Lung cancer, *Blumea balsamifera*

Introduction

Lung cancer is one of the most dangerous cancers that ranks second as the main cause of death globally, reaching 1.8 million death cases of 2.2 million patients per year.[1] According to WHO, lung cancer cases in Indonesia reached 30,023 new cases, with the number of deaths reaching 2.6% of the total population deaths in Indonesia per year.[2] Lung cancer is divided into two types, namely small cell lung cancer (SCLC), with an average number of cases of 20%, and non-small cell lung cancer (NSCLC), with a few cases reaching 80%.[1] NSCLC-type lung cancer has a more malignant nature with a higher metastatic potential.[3] One of the NSCLC models commonly used in basic lung cancer drug discovery research is A549 cell lines. A549 cells are a cell line derivative of alveolar type 2 (AT II) cells in human lung adenocarcinoma, which have been used quite widely in identifying the effects of a bioactive compound or the discovery of a new drug on the proliferation, apoptosis and metastasis of lung cancer cells.[4] As a type of lung cancer that has a high risk of treatment resistance, NSCLC requires more complex treatment or management.[5]

*Corresponding author. Email: rd.dinia@ub.ac.id
Tel: +62 813 2597 0829

Citation: Nurlailiyah FA, Dwijayanti DR, Hermanto FE, Masruri M, Widodo N. Cytotoxicity of *Blumea balsamifera* on A549 Lung Cancer Cells: Integrating *in Vitro* Analysis with Computational Study of AKT-1 Inhibition. Trop J Nat Prod Res. 2025; 9(2): 495 – 503 https://doi.org/10.26538/tjnpr/v9i2.12

Official Journal of Natural Product Research Group, Faculty of Pharmacy, University of Benin, Benin City, Nigeria

Lung cancer treatment is generally carried out with chemotherapy, radiotherapy, surgery, targeted therapy, and immunotherapy.[6] Current cancer treatment therapies are reported to have various side effects on the body, such as causing an increased risk of infection, fatigue, nausea, vomiting, diarrhea, and skin irritation.[7] Conventional therapy also has the potential to attack normal cells, causing the drug's mechanism of action to not act specifically on cancer cells, so new treatment strategies are needed that can induce cancer cell death with a minimum of side effects.[8] One strategy for treating cancer can be done by utilizing plant bioactive compounds.[9] Plants are commonly used in traditional medicine because they contain secondary metabolites that have biological activity, such as anticancer, so they can be developed in clinical drug preparations. The combination of herbal medicines from plants with conventional therapy has been reported to reduce side effects and the risk of complications caused by therapy.[10] Herbal medicines have gained considerable attention as potential anticancer agents due to their ability to selectively target cancer cells while minimizing damage to normal tissues. Many bioactive compounds derived from plants have demonstrated high specificity towards cancer cells by modulating oncogenic pathways that are often hyperactivated in malignancies. For instance, compounds like curcumin from *Curcuma longa* and artemisinin from *Artemisia annua* have been shown to selectively induce apoptosis in cancer cells by exploiting their heightened oxidative stress or dependency on survival pathways, sparing normal cells in the process.[11] This selective cytotoxicity has sparked interest in other medicinal plants, including *Blumea balsamifera* L., for their potential in cancer treatment.

B. balsamifera L., also known as the *Sembung Legi* in Indonesia, is one of the herbs that has been used in traditional medicine in several countries in Asia.[12] Bioactive compounds isolated from several parts of the *B. balsamifera* plant have been shown to have pharmacological activities including anti-inflammatory, antioxidant, hepatoprotective and anticancer effects.[13] *B. balsamifera* leaves are known to have the highest number of compounds with anticancer activity compared to

other parts. One of the main types of compounds found in *B. balsamifera* leaves are flavonoids, terpenoids and alkaloids.[14] Studies have demonstrated that its extracts exhibit significant cytotoxic effects against breast (MCF-7), cervical (HeLa), and colorectal (HCT116) cancer cells. These effects are primarily mediated through the induction of apoptosis, often through the mitochondrial pathway, and cell cycle arrest.[14] Given these findings, the bioactive compounds of *B. balsamifera* present a compelling avenue for further exploration as selective anticancer agents, potentially offering a therapeutic alternative that minimizes off-target effects on healthy cells.

The mechanism and application of the bioactive compounds from the ethanol extract of *B. balsamifera* plant leaves as an anti-lung cancer agent in A549 cells have not yet been carried out in a comprehensive manner. Thus, the anticancer of *B. balsamifera* will be explored using in vitro studies by WST-1 assay to determine the cytotoxicity effect of *B. balsamifera* leaves ethanol extract on the A549 lung cancer cells line. Furthermore, an in-silico study will be performed to find bioactive compounds of *B. balsamifera* and analyze the target proteins of these compounds in inhibiting the growth of lung cancer cells, shedding new light on the anticancer potential of *B. balsamifera*.

Materials and Methods

B. balsamifera leaves extraction

Dry powder of *B. balsamifera* leaves was purchased from UPT Materia Medica, Batu, Indonesia. The *microwave-assisted extraction* (MAE) method was used for powder extraction by dissolving in 96% ethanol in 1:10 ratio (herb: solvent) using some steps including holding temperature of 50°C, warming at 50°C for 5 mins, holding time of 50°C for 10 mins, and cooling down of 45°C for 5 mins. The *B. balsamifera* extract (BBE) was filtered using filter paper and evaporated using rotary vacuum evaporator (Buchi: Buchi R-210 Rotavapor System). The extract was freeze -dried until a dried extract was obtained.[15]

Cytotoxicity assay

The A549 cells as lung cancer cell line were purchased from JCRB Cell Bank. The cells were cultured on complete medium (MEM (Gibco) supplemented by 10% fetal bovine serum (Gibco) and 1% of antibiotic penicillin-streptomycin (Gibco) and incubated at 5% CO_2 and 37°C. The A549 cells were seeded on 96-well plates to approximately $7.5x10^3$ cells/well. The concentration of BBE used were 0, 50, 100, and 200 µg/mL then the cells were treated for 24 hours. The cytotoxicity activity of BBE was analyzed using WST-1 (Sigma) with 5% concentration (v/v medium). The absorbance was measured using an ELISA reader (BioTek ELx808) at a wavelength of 450 nm.[15]

Statistical analysis

The data were analyzed using a t-test to assess differences between the control and the extract doses, with a *p*-value < 0.05 and < 0.01 indicating statistical significance.

Bioactive compounds of B. balsamifera data mining

The compounds contained in *B. balsamifera* leaves were obtained from previous studies that focused on active compounds that were isolated using ethanol extract solvent.[13,15] Canonical SMILES and the three-dimensional (3D) structure of the compound contained in BBE were obtained from the PubChem database (https://pubchem.ncbi.nlm.nih.gov/).

Screening bioactive compounds based on probable activity

The compounds contained in *B. balsamifera* leaves from the database were selected by screening for possible activities. This method was conducted to select the compounds that have a function to interact with pathway signaling in the A549 cells using the PASS Online webserver (https://www.way2drug.com/pass online/).[16] The pathway activity was selected based on their function as anti-lung cancer agents, such as anticarcinogenic, chemo-preventive, proliferative disease treatment, JAK2 expression inhibitor, TP53 expression enhancer, chemoprotective, apoptosis agonist, caspase-3 stimulant, caspase-8 stimulant, MMP9 expression inhibitor, antineoplastic (lung cancer), dan Bcl2 antagonist.

Protein target prediction

The compounds that pass the probable activities screening were used for target protein prediction using SWISS Target Prediction database (https://www.swiss targetprediction.ch/). SwissTargetPrediction is a webserver to accurately predict the direct target protein based on the similarity of compound structure to a previously known compound.[17] The results obtained were summarized and visualized using Microsoft Excel 2021 software in bar chart form, then a protein that most related to lung cancer were taken.

Molecular docking

Molecular docking was conducted between the compound as ligand and target protein as receptor. The three-dimensional (3D) structure of the compound contained in BBE was obtained from the PubChem database then prepared using OpenBabel integrated into the PyRx software. The protein's 3D structure of RAC-alpha serine/threonine-protein kinase (AKT1) was obtained from the RCSB PDB database (https://www.rcsb.org/) with PDB ID 4EJN.[18] The contaminant ligands and water molecules were removed using Biovia Discovery Studio 2019 software (Dassault Systemes Biovia, San DIeego, CA, USA). Docking was performed using AutoDock Vina in PyRx 0.8,[19] targeting the AKT1 active site with grid box settings detailed in Table 1, as referenced in a prior study.[18] Docking results were visualized with Biovia Discovery Studio 2019.

Table 1: Grid box setting to target the active site of AKT1 in this study

Vina Search Space	Axis		
	X	Y	Z
Center (Å)	35.6910577775	43.3205961196	18.2444772814
Size (Å)	22.5867738837	22.2661159006	25.4736749463

Molecular dynamics simulation

Molecular dynamic simulation was conducted using the YASARA (Yet Another Scientific Artificial Reality Application) software[20] with the AMBER14 force field.[21] The system conditions were adjusted according physiological condition of the cells (310K, pH 7.4, 1 atm, and 0.9% salt content) for 20 ns.[15] The duration of 20 ns is considered a suitable duration for RMSD analysis because it provides a sufficient sampling of the complex's dynamics to accurately assess its stability and interactions. This duration allows for a detailed analysis of the protein-ligand complex's behavior over time, including the detection of metastable states and the characterization of stable states. Additionally, this duration is enough to average out any transient fluctuations, giving a more accurate representation of the complex's dynamics.

Results and Discussion

Cytotoxicity of B. balsamifera leaves ethanol extract to A549 lung cancer cell line

The cytotoxic effect of BBE on the A549 lung cancer cell line with WST-1 reagent was carried out using variations of extract dose, including 0, 50, 100, and 200 µg/mL. As shown in Figure 1, BBE excellently reduced the viability of A549 cells in a dose-dependent manner. The statistical analysis showed a significant difference ($p < 0.05$) at doses of 100 µg/mL and 200 µg/mL when compared with the control. The IC_{50} value for BBE against A549 cells is 124.92 ± 13.24 µg/mL, indicating that this concentration can reduce the population of living lung cancer cells by 50%.

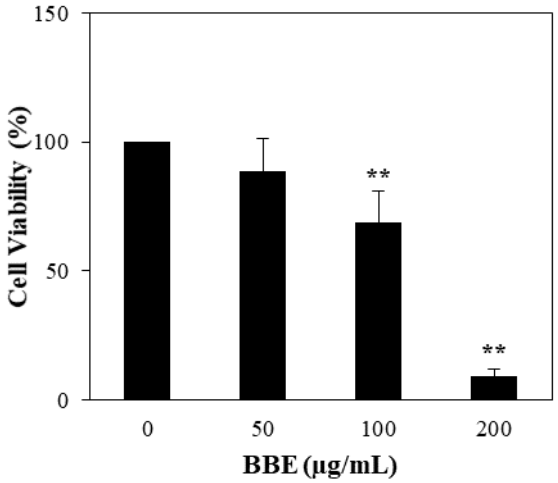

Figure 1: Analysis of A549 cell viability after administration of BBE at doses of 0 (control), 50, 100, and 200 µg/mL revealed a significant dose-dependent decrease in cell viability compared to the control group. Asterisk (**) symbol indicates a significant difference with control group with p value < 0.01.

Bioactive compound contained in Ethanol Extract of B. balsamifera Leaves

According to previous studies and the PubChem database,[13,15] 20 bioactive compounds were identified in *B. balsamifera* leaves (Table 2). These include dihydroflavonoids (3 compounds), flavonoids (3 compounds), flavonols (5 compounds), and single representatives from the phenol, monoterpenoid, and steroid groups.

Anti-Lung Cancer Potential and Probable Protein Targets of B. balsamifera's Bioactive Compounds

By using structure-activity relationship (SAR) analysis in PASS Online Webserver, *B. balsamifera* leaf compounds were assessed for their probable activity (Pa) to predict potential bioactivity against lung cancer. Twenty bioactive compounds from previous data were evaluated on a Pa scale ranging from 0 to 1 (Figure 2a). The analysis identified 11 promising compounds (Figure 2c) with Pa values suggesting their potential bioactivity to inhibit NSCLC development across multiple bioactivity parameters. Compounds with Pa values below 0.3 in more than four parameters were excluded, focusing only on the most viable candidates. The potential mechanisms of action for these 11 compounds were further explored using the SwissTarget Prediction tool to identify their protein targets.

Table 2. Bioactive compounds in B. balsamifera leaves from the previous studies and PubChem database

No	Compound	Group of Compounds	CID	Formula	MW (g/mol)	Ref.
1	Eriodictyol	Dihydroflavonoid	440735	$C_{15}H_{12}O_6$	228.25	[13]
2	Liquiritigenin	Dihydroflavonoid	114829	$C_{15}H_{12}O_4$	256.25	[13]
3	Catechin	Flavonoid	9064	$C_{15}H_{14}O_6$	290.26	[12]
4	Ombuin	Flavonol	5320287	$C_{17}H_{14}O_7$	330.29	[13]
5	Ayanin	Flavonol	5280682	$C_{18}H_{16}O_7$	344.31	[13]
6	Rutin	Flavonol	5280805	$C_{27}H_{30}O_{16}$	610.52	[12]
7	Luteolin	Flavonoid	5280445	$C_{15}H_{10}O_6$	286.24	[12]
8	Xanthoxylin	Phenol	66654	$C_{10}H_{12}O_4$	196.19	[12]
9	Quercetin	Flavonol	5280343	$C_{15}H_{10}O_7$	302.24	[12]
10	Rhamnetin	Flavonoid	5281691	$C_{16}H_{12}O_7$	316.26	[13]
11	Tamarixetin	Flavonol	5281699	$C_{16}H_{12}O_7$	316.27	[13]
12	Borneol	Monoterpenoid	1201518	$C_{10}H_{18}O$	154.25	[12]
13	Blumealactone	Sesquiterpene	162916296	$C_{17}H_{24}O_6$	364.43	[13]
14	Blumeatin	Dihydroflavonoid	70696494	$C_{16}H_{14}O_6$	302.28	[12]
15	Blumeaene	Sesquiterpene	52936861	$C_{20}H_{30}O_6$	366.40	[13]
16	Samboginone	Sesquiterpene	52936973	$C_{15}H_{22}O_3$	250.34	[12]
17	Cryptomeridiol	Sesquiterpene	165258	$C_{15}H_{28}O_2$	240.39	[13]
18	Sterebin A	Diterpenoid	21681091	$C_{18}H_{30}O_4$	310.43	[13]
19	Austroinulin	Diterpenoid	11472742	$C_{20}H_{34}O_3$	322.49	[13]
20	Stigmasterol	Steroid	5280794	$C_{29}H_{48}O$	412.69	[13]

CID: compound identity

This analysis revealed 12 proteins associated with NSCLC development targeted by the compounds. Notably, AKT1 emerged as the most frequently targeted protein, with 10 of the 11 compounds interacting with it (Figure 2b). Therefore, AKT-1 was selected as the protein target for subsequent analysis.

Interaction of Screened Compounds Towards AKT-1

The molecular docking analysis revealed that the inhibitor (control) had the lowest binding affinity at -13.26 kcal/mol, indicating its strong interaction with the AKT-1 receptor. Among the tested compounds, the three with the next lowest binding affinities were rutin (-10.88 kcal/mol), eriodictyol (-9.61 kcal/mol), and ombuin (-9.58 kcal/mol). These compounds demonstrated significant potential as ligands, with rutin showing the closest binding energy to the inhibitor (Table 3).

ISSN 2616-0684 (Print)
ISSN 2616-0692 (Electronic)

Table 3. Comparison of binding affinity and interactions between control ligands and *B. balsamifera* leaf compounds with AKT-1 protein

No	Ligand	Binding Affinity (kcal/mol)	Interactions		
			Hydrogen Bonds	Hydrophobic Bonds	Van der Waals
1	Inhibitor Compound (control)	-13,26	**ASN54, TRP80, THR211, ILE290**	**GLN79, ILE84, LEU210, LEU264, VAL270, TYR272, ARG273, ASP292**	**ASN53, GLN59, LEU78, THR82, VAL271, ASP274, ILE290, THR291, TYR326**
2	Rutin	-10,88	**ASN54**, **GLN59**, **LEU78**, **GLN79**, SER205, **THR211**, **THR82**	**TRP80**, LEU202, **LEU210**, **LEU264**, **VAL270**, **ASP292**	**ASN53**, **THR82**, **ILE84**, VAL201, GLN203, ALA212, LYS268
3	Eriodictyol	-9,61	**ASN54**, SER205, **THR211**	**TRP80**, **LEU210**	**THR82**, **ILE84**, GLN203, ASN204, **LEU264**, LYS268, **VAL270**, **TYR272**, **ASP292**
4	Ombuin	-9,58	**GLN79**, **THR82**, SER205, **TYR272**, **ASP292**	**TRP80**, **LEU210**, **LEU264**	**ILE84**, LYS268, **VAL270**, **VAL271**, **ARG273**
5	Blumeatin	-9,57	**ASN54**, SER205, **THR211**	**TRP80**, **LEU210**, **LEU264**	**THR82**, **ILE84**, LYS268, **VAL270**, **TYR272**, **ASP292**
6	Luteolin	-9,46	**ASN54**, SER205, **THR211**	**GLN79**, **TRP80**, **LEU210**, **LEU264**, **VAL270**	**ILE84**, ALA212, ASN204, LYS268, **TYR272**
7	Tamarixetin	-9,42	**ASN54**, **THR82**, **THR211**, **TYR272**	**TRP80**, **LEU264**, **ASP292**	**ILE84**, SER205, **LEU210**, LYS268, **VAL270**, VAL271, **ARG273**
8	Rhamnetin	-9,41	**GLN79**, SER205, **THR211**, **VAL271**	**TRP80**, **LEU210**, **LEU264**, **ASP292**	**ASN54**, THR81, **THR82**, **ILE84**, ASN204, LYS268, **VAL270**, **TYR272**, **ARG273**, **THR291**
9	Quercetin	-9,36	SER205, **VAL271**	**TRP80**, **LEU210**	THR81, **THR82**, **ILE84**, ASN204, **THR211**, LYS268, **VAL270**, **TYR272**, **ARG273**
10	Catechin	-9,26	**ASN54**, **THR82**, SER205, **THR211**, **ASP292**	**TRP80**, **LEU210**, **LEU264**	**ILE84**, ALA212, LYS268, **VAL270**, **VAL271**, **TYR272**
11	Ayanin	-9,25	**ASN54**, **VAL271**, **TYR272**	**TRP80**, **LEU264**, LYS268, **VAL270**	ASN53, **GLN79**, THR81, **THR82**, **ILE84**, ASN204, SER205, **LEU210**, **ARG273**, **ASP274**, **ASP292**
12	Liquiritigenin	-8,99	SER205, **THR211**	**TRP80**, **LEU210**, **TYR272**	**ASN54**, **GLN79**, **THR82**, **ILE84**, GLN203, ASN204, **LEU264**, **VAL270**, **VAL271**, **ARG273**, **ASP292**

Amino acid residues in bold: interaction of the same residue as the inhibitor compound (control); blue column: AKT-1 ligand-protein complex with the best binding affinity

Rutin displayed substantial overlap in residue interactions with the inhibitor, including critical residues such as ASN54, TRP80, and THR211. This overlap, along with its high binding affinity, suggests that rutin closely mimics the interaction pattern of the inhibitor. Similarly, eriodictyol interacted with residues like ASN54, SER205, and TRP80, indicating some similarity to the inhibitor's binding sites. Ombuin, while slightly weaker in binding energy than eriodictyol, shared interactions at residues such as TRP80, LEU210, and TYR272, reflecting a moderate resemblance to the inhibitor's interaction profile (Figure 3 and Table 3). Among the top three compounds, rutin stood out due to its stronger binding affinity and higher degree of overlap with the inhibitor's binding residues. While eriodictyol and ombuin also showed promise, their interaction patterns were less similar to the inhibitor. However, additional experimental validation and molecular dynamics simulations are required to confirm their potentials as an effective AKT-1 inhibitor.

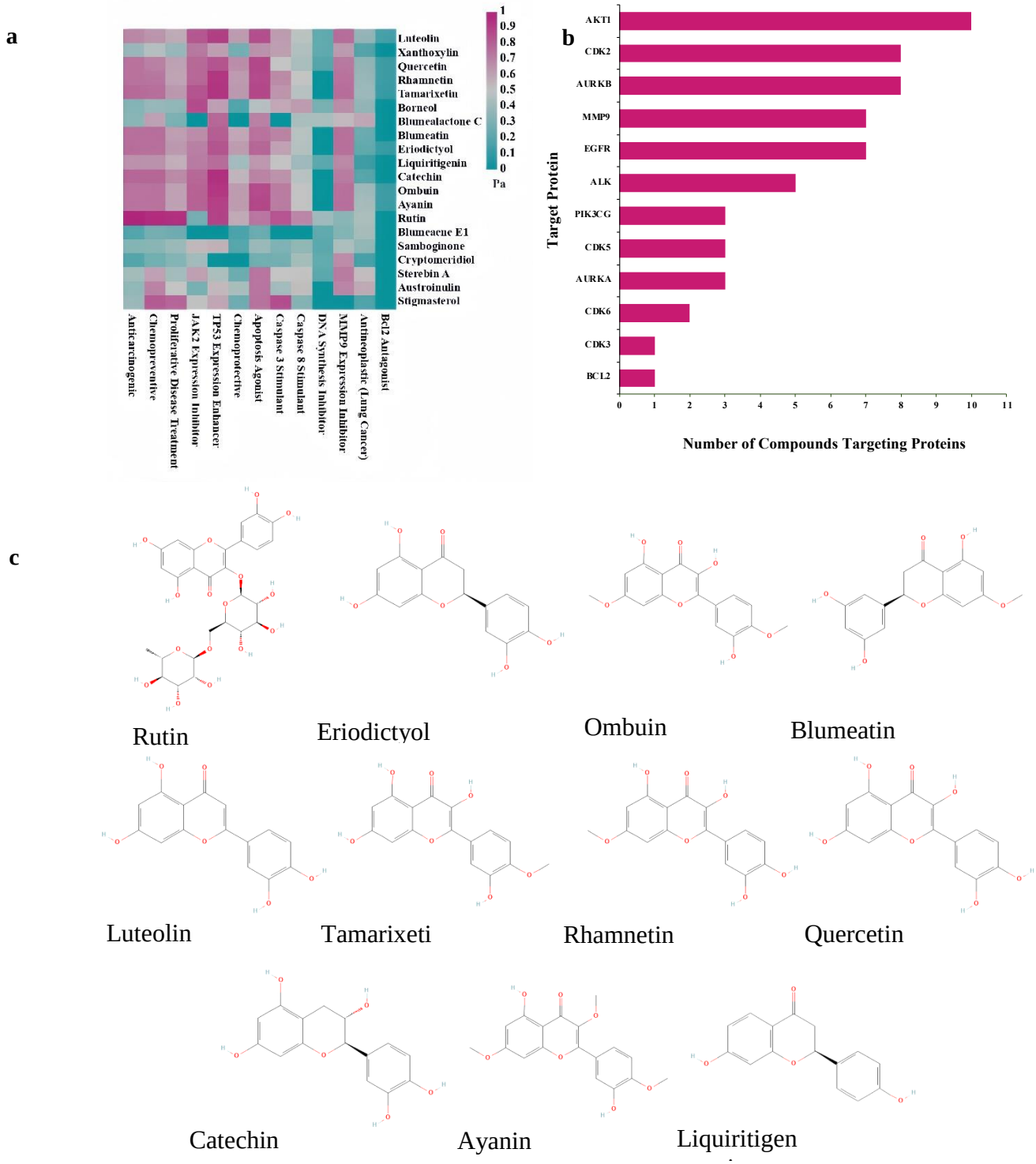

Figure 2: Screening of bioactive compounds from BEE identified several potential protein targets and compounds with anticancer properties. (a) Heatmap illustrating the bioactivity of compounds against various targets. (b) Bar chart showing the distribution of compounds targeting different proteins. (c) Chemical structures of the 11 compounds exhibiting probable activity.

Molecular dynamic simulation

Figure 4 illustrates the molecular dynamics simulations, highlighting the structural stability and interaction dynamics of the AKT-1 protein complexed with the inhibitor (control) and three bioactive compounds from BEE: rutin, eriodictyol, and ombuin. The analysis of hydrogen bond formation revealed that the rutin-AKT-1 complex consistently maintained the highest number of hydrogen bonds, indicating strong and stable interactions throughout the 20 ns simulation. The inhibitor (control) followed with a moderate yet stable number of hydrogen bonds, while eriodictyol and ombuin showed fewer hydrogen bonds (Figure 4a). The backbone RMSD of backbone atoms analysis showed minimal fluctuations for all complexes, confirming structural stability across the simulation period (Figure 4b).

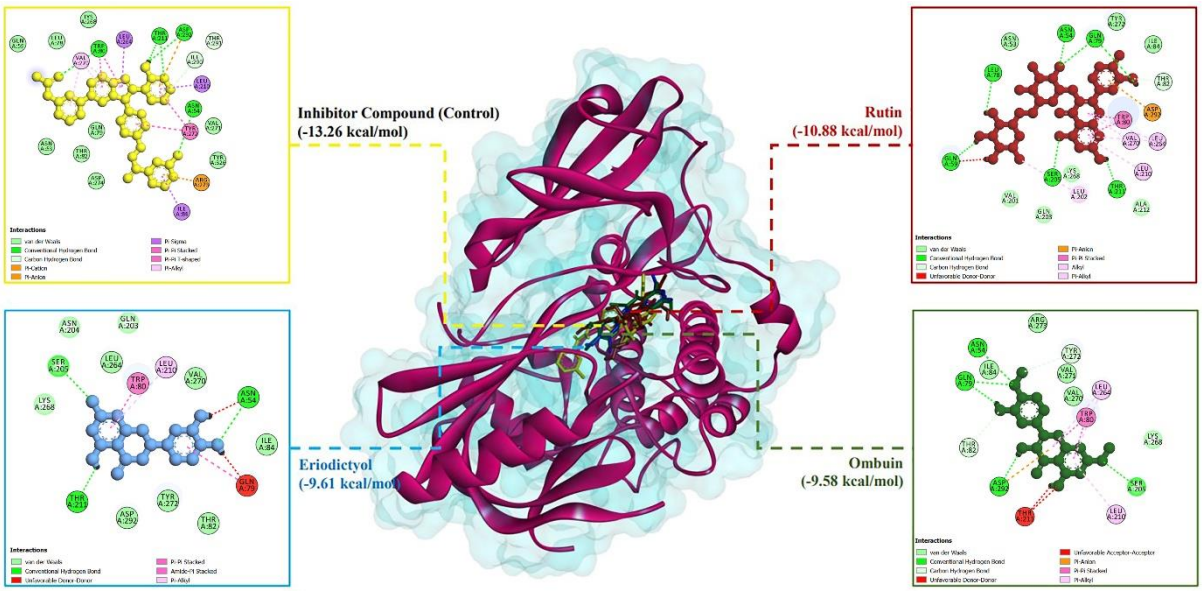

Figure 3: Binding interactions of inhibitor compound and selected compounds from BBE with the AKT-1 protein receptor, predicted through molecular docking. Binding energies are indicated for each ligand.

Ligand movement RMSD demonstrated that eriodictyol exhibited the least movement, reflecting higher binding stability. The inhibitor displayed slightly greater movement than eriodictyol, while ombuin showed the highest fluctuation, although still within acceptable stability thresholds. Rutin initially exhibited a slight increase in movement at the start of the simulation but later stabilized, forming a strong complex with AKT-1 (Figure 4c). Residue-level fluctuations indicated lower RMSF values for the inhibitor and eriodictyol, while ombuin caused notable fluctuations, particularly at residues ARG144, VAL201, and LYS301. Rutin displayed moderate fluctuations, primarily at LYS301, but overall retained significant stability (Figure 4d). The cytotoxicity of the ethanol extract of BBE on A549 lung cancer cells was classified as moderate based on its IC50 value, aligning with the National Cancer Institute's classification system (≤ 20 µg/mL: strong; 21–200 µg/mL: moderate; 201–500 µg/mL: low; > 501 µg/mL: no cytotoxic effect).[22] As shown in Figure 1, a dose-dependent decrease in cell viability was observed, confirming BBE's moderate cytotoxic effect. These results gave better results than previous study, which mention that BBE has IC50 value at around 345 µg/mL, although still considered as the same moderate toxicity category.[23] However, fractionation of BBE with ethyl acetate gave better results, and some compounds from ethyl acetate fraction showed strong inhibitory activity than crude extract.[23] Despite its known anti-lung cancer activity, a precise mechanism of BBE against lung cancer remains unknown. Thus, this study employed *in silico* analysis to elucidate a potential mechanism of BBE towards lung cancer cytotoxicity. Across through 20 bioactive compounds, 11 compounds were screened for potential inhibitory activity against predicted protein target, AKT-1, according to the screening of SAR of PASS Online and SwissTarget Prediction (Figure 2). The occurrence of AKT-1 as prominent target in this study is not surprising, since its major role in development of various cancer cells and frequently targeted to achieved anti-cancer mechanisms. Inhibiting AKT-1 showed a potential anti-cancer activity across multiple cancers.[24] Therefore, this study will also uncover a potential anti-lung cancer activity of BBE through AKT-1 inhibition.

Molecular docking analysis of AKT-1 showed that the inhibitor (control) interacts with critical residues TRP80, SER205, and VAL270, aligning with experimental findings.[18] However, residues such as MET227, TYR229, and LYS268, identified experimentally,[18] were not observed in the docking results. TRP80 and VAL270, within the hydrophobic cluster of the AKT-1 ATP-binding cleft, are crucial for stabilizing the kinase's inactive state by maintaining its autoinhibitory conformation.[18] Targeting these residues offers a selective and potentially less toxic approach to AKT-1 inhibition without competing with ATP.[18] Among the screened compounds, rutin, eriodictyol, and ombuin demonstrated the best binding affinities for AKT-1 (Table 3, Figure 3). These compounds not only closely resembled the inhibitor's docking profile but also interacted with several experimentally validated key residues.[18] Rutin engaged TRP80, SER205, LYS268, and VAL270, closely mirroring the inhibitor's binding. Similarly, eriodictyol targeted TRP80, SER205, LYS268, and VAL270, showing strong alignment with the essential binding site. Ombuin also interacted with these key residues but uniquely targeted TYR272 instead of TYR229, which may slightly alter its binding dynamics without reducing efficacy. Hence, rutin and eriodictyol closely mimic the inhibitor's binding pattern, while ombuin, despite minor differences, effectively targets key residues, emphasizing its potential to stabilize AKT-1 in its inactive state. Molecular dynamics simulations confirmed the binding stability of rutin, eriodictyol, and ombuin with AKT-1 (Figure 4). Rutin exhibited the highest number of hydrogen bonds, demonstrating stable interactions with AKT-1 as displayed in ligand movement RMSD.[25] Ombuin showed significant fluctuation in ligand movement RMSD. RMSF revealed significant variability in ARG144, VAL201, and LYS301. As these residues are not critical for inhibitor binding or enzyme activity, their fluctuations are unlikely to impact protein-ligand stability.[26] Notably, VAL201 interacts with rutin through Van der Waals forces, though this interaction is dispensable given the transient nature of such forces.[27] Overall, the simulations demonstrated consistent hydrogen bond counts, low backbone RMSD values, and minimal ligand movement, indicating stable protein-ligand interactions.[15,28]

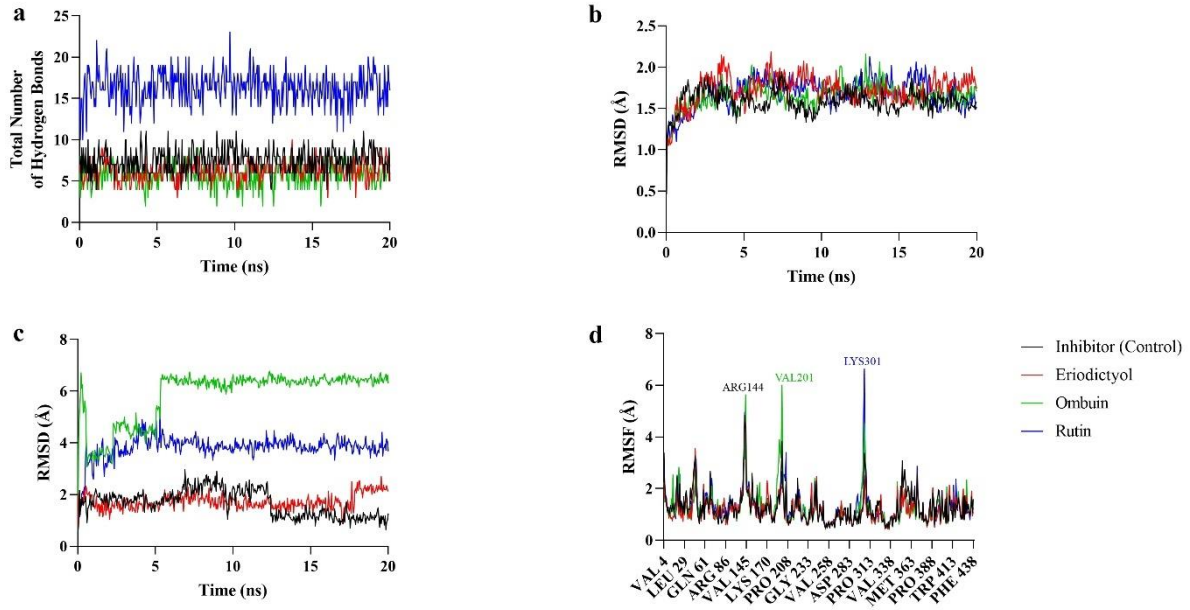

Figure 4: Molecular dynamics simulation of AKT-1 complexed with the inhibitor (control), rutin, eriodictyol, and ombuin. (a) Hydrogen bond count, (b) backbone RMSD, (c) ligand movement RMSD, and (d) residue-level fluctuations (RMSF) highlight the stability and interaction dynamics.

AKT-1 protein kinase plays a pivotal role in lung cancer pathogenesis by regulating critical processes such as cell proliferation, survival, and metastasis through the PI3K/AKT/mTOR signaling pathway, which is often hyperactivated in NSCLC.[29] AKT-1 facilitates tumor growth by promoting cell cycle progression, inhibiting cyclin-dependent kinase inhibitors, and enhancing cyclin expression, enabling the G1 to S phase transition.[30] It also supports cell survival by phosphorylating and inactivating pro-apoptotic factors like BAD and caspase-9 while upregulating anti-apoptotic proteins such as B-cell lymphoma-2 (BCL-2) and Myeloid leukemia 1 (MCL-1).[31] Furthermore, AKT-1 enhances metastasis by driving epithelial-mesenchymal transition (EMT), characterized by reduced cell adhesion, increased motility, and elevated EMT marker expression, such as N-cadherin and Vimentin.[29,32] Targeting AKT-1 offers a promising therapeutic strategy to combat lung cancer by disrupting these oncogenic processes. Inhibiting AKT-1 triggers apoptosis by activating pro-apoptotic pathways and reducing the phosphorylation of survival-promoting factors.[33,34] It also induces cell cycle arrest at the G1 phase by downregulating cyclins and CDKs critical for cell cycle progression.[35,36] Additionally, AKT-1 inhibition can activate alternative cell death pathways, including autophagy and necrosis, often mediated by reactive oxygen species (ROS) production.[33,37] Understanding these mechanisms highlights the therapeutic potential of AKT-1 inhibition and underscores its importance in developing targeted treatments for lung cancer. This study provides novel insights into the anticancer potential of BBE's compounds. While rutin's ability to modulate AKT-1 has been recognized,[38] this is the first report detailing its inhibitory activity towards AKT-1 protein, specifically in lung cancer. Similarly, although eriodictyol has been associated with disrupting the m-TOR/PI3K/AKT signaling pathway in A549 cells,[39] its direct interaction with AKT-1 is explored here for the first time. Finally, this research uniquely identifies ombuin as a potential AKT-1 inhibitor in lung cancer, making it the first to propose its role in targeting this protein. These findings underscore the unique position of this study in advancing natural compound-based strategies for anti-lung cancer therapy through AKT-1 inhibition.

Conclusion

The BEE exhibited moderate cytotoxicity against A549 lung cancer cells, with an IC50 of 124.92 ± 13.24 µg/mL. *In silico* studies support this observation, suggesting that BEE exerts its anticancer effects by inhibiting proteins involved in cancer cell growth and survival, particularly AKT-1. Among the active compounds identified in BEE, rutin, eriodictyol, and ombuin demonstrated the strongest potential as anti-lung cancer agents due to their robust and stable interactions with AKT-1.

Conflict of Interests

There are no competing interests for any of the authors.

Authors' Declaration

The authors hereby declare that the work presented in this article are original and that any liability for claims relating to the content of this article will be borne by them.

Acknowledgment

The researchers express their gratitude to the Animal Physiology Laboratory, Department of Biology, Universitas Brawijaya, for their support during this study. Appreciation is also extended to the High-Performance Computing (HPC) facility from AI-Center UB for providing the necessary computational resources. This work was financially supported by DRTPM (Directorate General of Higher Education, Ministry of Education and Culture, Republic of Indonesia) under the Penelitian Fundamental Reguler (PFR) scheme (Grant No. 045/E5/PG/02/00/PL/2024).

References

1. Nahar J, Boopathi V, Murugesan M, Rupa EJ, Yang DC, Kang SC, Mathiyalagan R. Investigating the Anticancer Activity of G-Rh1 Using *In Silico* and *In Vitro* Studies (A549 Lung Cancer Cells). Molecules. 2022;27(23): 8311. doi:10.3390/molecules27238311.
2. Suraya A, Nowak D, Sulistomo AW, Icksan AG, Berger U, Syahruddin E, Bose-O'Reilly S. Excess risk of lung cancer among agriculture and construction workers in Indonesia. Ann Glob Health. 2021;87(1): 8. doi:10.5334/aogh.3155.
3. Zheng M. Classification and pathology of lung cancer. Surg Oncol Clin. 2016;25(3): 447-468. doi:10.1016/j.soc.2016.02.003.
4. Garcia-de-Alba C. Repurposing A549 adenocarcinoma cells: new options for drug discovery. Am J Respir Cell Mol Biol. 2021;64(4): 405-406. doi:10.1165/rcmb.2021-0048ED.

5. Simpson KL, Stoney R, Frese KK, Simms N, Rowe W, Pearce SP, Humphrey S, Booth L, Morgan D, Dynowski M, Trapani F. A biobank of small cell lung cancer CDX models elucidates inter- and intratumoral phenotypic heterogeneity. Nat Cancer. 2020;1(4): 437-451. doi:10.1038/s43018-020-0046-2.
6. Girigoswami A, Girigoswami K. Potential applications of nanoparticles in improving the outcome of lung cancer treatment. Genes. 2023;14(7): 1370. doi:10.3390/genes14071370.
7. Islam KM, Anggondowati T, Deviany PE, Ryan JE, Fetrick A, Bagenda D, Copur MS, Tolentino A, Vaziri I, McKean HA, Dunder S. Patient preferences of chemotherapy treatment options and tolerance of chemotherapy side effects in advanced stage lung cancer. BMC cancer. 2019;19(1): 835. doi:10.1186/s12885-019-6054-x.
8. Xu P, Le Pechoux C. Chemoradiotherapy for stage III non-small cell lung cancer: have we reached the limit?. China Clin Oncol. 2015;4(4): 45. doi:10.3978/j.issn.2304-3865.2015.11.04.
9. Safarzadeh E, Shotorbani SS, Baradaran B. Herbal medicine as inducers of apoptosis in cancer treatment. Adv Pharm Bull. 2014;4(1): 421. doi:10.5681/apb.2014.062.
10. Sulaiman C, George BP, Balachandran I, Abrahamse H. Photoactive herbal compounds: a green approach to photodynamic therapy. Molecules. 2022;27(16): 5084. doi:10.3390/molecules27165084.
11. Shrihastini V, Muthuramalingam P, Adarshan S, Sujitha M, Chen JT, Shin H, Ramesh M. Plant derived bioactive compounds, their anti-cancer effects and *in silico* approaches as an alternative target treatment strategy for breast cancer: An updated overview. Cancers. 2021;13(24): 6222. doi:10.3390/cancers13246222.
12. Masyudi M, Hanafiah M, Rinidar R, Usman S, Marlina M. Phytochemical screening and GC-MS analysis of bioactive compounds of *Blumea balsamifera* leaf extracts from South Aceh, Indonesia. Biodiversitas. 2022;23(3): 1344-1352. doi:10.13057/biodiv/d230319.
13. Pang Y, Wang D, Fan Z, Chen X, Yu F, Hu X, Wang K, Yuan L. *Blumea balsamifera*—A phytochemical and pharmacological review. Molecules. 2014;19(7): 9453-9477. doi:10.3390/molecules19079453.
14. Wang J, He H, Zhou Z, Bai L, She X, He L, He Y, Tan D. Chemical constituents and bioactivities of *Blumea balsamifera* (Sembung): a systematic review. Food Sci Technol. 2023;43: e132322. doi:10.1590/fst.132322.
15. Marseti SW, Hermanto FE, Widyananda MH, Rosyadah N, Kamila FS, Annisa Y, Dwijayanti DR, Ulfa SM, Widodo N. Pharmacological potential of *Clinacanthus nutans*: integrating network pharmacology with experimental studies against lung cancer. J Biol Active Prod Nat. 2024;14(3): 343-358. doi:10.1080/22311866.2024.2367997.
16. Filimonov DA, Lagunin AA, Gloriozova TA, Rudik AV, Druzhilovskii DS, Pogodin PV, Poroikov VV. Prediction of the biological activity spectra of organic compounds using the PASS online web resource. Chem Heterocycl Compd. 2014;50: 444-457. doi:10.1007/s10593-014-1496-1.
17. Gfeller D, Grosdidier A, Wirth M, Daina A, Michielin O, Zoete V. SwissTargetPrediction: a web server for target prediction of bioactive small molecules. Nucleic Acids Res. 2014;42(1): 32-38. doi:10.1093/nar/gku293.
18. Ashwell MA, Lapierre JM, Brassard C, Bresciano K, Bull C, Cornell-Kennon S, Eathiraj S, France DS, Hall T, Hill J, Kelleher E. Discovery and optimization of a series of 3-(3-Phenyl-3 H-imidazo [4, 5-b] pyridin-2-yl) pyridin-2-amines: orally bioavailable, selective, and potent ATP-independent Akt inhibitors. J Med Chem. 2012;55(11): 5291-5310. doi:10.1021/jm300276x/
19. Dallakyan S, Olson AJ. Small-molecule library screening by docking with PyRx. Chem Biol Methods Protocols. 2015: 243-250. doi:10.1007/978-1-4939-2269-7_19.
20. Krieger E, Vriend G. New ways to boost molecular dynamics simulations. J Comput Chem. 2015;36(13): 996-1007.doi:10.1002/jcc.23899.
21. Maier JA, Martinez C, Kasavajhala K, Wickstrom L, Hauser KE, Simmerling C. ff14SB: improving the accuracy of protein side chain and backbone parameters from ff99SB. J Chem Theory Comput. 2015;11(8): 3696-3713. doi:10.1021/acs.jctc.5b00255.
22. Srisawat T, Chumkaew P, Heed-Chim W, Sukpondma Y, Kanokwiroon K. Phytochemical screening and cytotoxicity of crude extracts of *Vatica diospyroides* symington type LS. Trop J Pharm Res. 2013;12(1): 71-76. doi:10.4314/tjpr.v12i1.12.
23. Saewan N, Koysomboon S, Chantrapromma K. Anti-tyrosinase and anti-cancer activities of flavonoids from *Blumea balsamifera* DC. J Med Plants Res. 2011;5(6): 1018-1025. doi:10.5897/JMPR.9000112.
24. Hassan D, Menges CW, Testa JR, Bellacosa A. AKT kinases as therapeutic targets. J Exp Clin Cancer Res. 2024;43(1):313. doi:10.1186/s13046-024-03207-4.
25. Syahraini A, Harnelly E, Hermanto FE. Pro-Apoptosis Activity of Pogostemon cablin Benth. Against Nasopharyngeal Carcinoma through the BCL-2 Inhibition Signaling Pathway: A Computational Investigation. Makara J Sci. 2023;27(3):6. doi:10.7454/mss.v27i3.1484.
26. Susilo A, Cahyati M, Nurjannah N, Pranowo D, Hermanto FE, Primandasari EP. Chrysin Inhibits Indonesian Serotype Foot-and-Mouth-Disease Virus Replication: Insights from DFT, Molecular Docking and Dynamics Analyses. J Trop Biodivers Biotechnol. 2024;9(1): 83140. doi:10.22146/jtbb.83140.
27. Song X, Zhao X. The van der Waals interaction between protein molecules in an electrolyte solution. J Chem Phys. 2004;120(4): 2005-2009. doi:10.1063/1.1634955
28. Fatchiyah F, Hermanto FE, Virgirinia RP, Rohmah RN, Triprisila LF, Suyanto E, Miyajima K. Inhibition of adipocyte senescence by ferulic acid present in pigmented rice through the PPAR-γ and NF-κB protein signaling pathways. J Pharm Pharmacogn Res. 2025;13(2): 402-415. doi:10.56499/jppres24.2080_13.2.402.
29. Moghbeli M. PI3K/AKT pathway as a pivotal regulator of epithelial-mesenchymal transition in lung tumor cells. Cancer Cell Int. 2024;24(1): 165. doi:10.1186/s12935-024-03357-7.
30. Sizek H, Hamel A, Deritei D, Campbell S, Ravasz Regan E. Boolean model of growth signaling, cell cycle and apoptosis predicts the molecular mechanism of aberrant cell cycle progression driven by hyperactive PI3K. PLoS Comput Biol. 2019;15(3): e1006402.doi:10.1371/journal.pcbi.1006402.
31. Coloff JL, Macintyre AN, Nichols AG, Liu T, Gallo CA, Plas DR, Rathmell JC. Akt-dependent glucose metabolism promotes Mcl-1 synthesis to maintain cell survival and resistance to Bcl-2 inhibition. Cancer res. 2011;71(15): 5204-5213. doi:10.1158/0008-5472.can-10-4531.
32. Grille SJ, Bellacosa A, Upson J, Klein-Szanto AJ, Van Roy F, Lee-Kwon W, Donowitz M, Tsichlis PN, Larue L. The protein kinase Akt induces epithelial mesenchymal transition and promotes enhanced motility and invasiveness of squamous cell carcinoma lines. Cancer res. 2003;63(9):2172-2178.
33. Zhang Y, Zhang C, Li J, Jiang M, Guo S, Yang G, Zhang L, Wang F, Yi S, Wang J, Fu Y. Inhibition of AKT induces p53/SIRT6/PARP1-dependent parthanatos to suppress tumor growth. Cell Commun Signal. 2022;20(1): 93. doi:10.1186/s12964-022-00897-1.
34. Li X, Fu Y, Xia X, Zhang X, Xiao K, Zhuang X, Zhang Y. Knockdown of SP1/Syncytin1 axis inhibits the proliferation and metastasis through the AKT and ERK1/2 signaling pathways in non-small cell lung cancer. Cancer Med. 2019;8(12): 5750-5759. doi:10.1002/cam4.2448.
35. Zhang C, Zhao X, Wang Z, Gong T, Zhao H, Zhang D, Niu Y, Li X, Zhao X, Li G, Dong X. Dasatinib in combination with BMS-754807 induce synergistic cytotoxicity in lung cancer cells through inhibiting lung cancer cell growth, and inducing autophagy as well as cell cycle arrest at the G1 phase. Invest New Drugs. 2023;41(3): 438-452. doi:10.1007/s10637-023-01360-9.
36. Lal M, Bae D, Patierno S, Ceryak S. The role of Akt1 in G1/S checkpoint bypass after genotoxin exposure. Cancer Res. 2008;68(9):5583.

37. Huang Y, Huang Y, Zhu G, Zhang B, Zhu Y, Chen B, Gao X, Yuan J. A Meroterpenoid from Tibetan medicine induces lung cancer cells apoptosis through ROS-mediated inactivation of the AKT pathway. Molecules. 2023;28(4): 1939. doi:10.3390/molecules28041939.
38. Nouri Z, Fakhri S, Nouri K, Wallace CE, Farzaei MH, Bishayee A. Targeting multiple signaling pathways in cancer: The rutin therapeutic approach. Cancers. 2020;12(8): 2276. https://doi.org/10.3390/cancers12082276.
39. Zhang Y, Zhang R, Ni H. Eriodictyol exerts potent anticancer activity against A549 human lung cancer cell line by inducing mitochondrial-mediated apoptosis, G2/M cell cycle arrest and inhibition of m-TOR/PI3K/Akt signalling pathway. Arch Med Sci. 2020;16(2): 446-452.doi:10.5114/aoms.2019.85152.